Secreted human glycyl-tRNA synthetase implicated in defense against ERK-activated tumorigenesis

Min Chul Park[a], Taehee Kang[a], Da Jin[a], Jung Min Han[a], Sang Bum Kim[a], Yun Jung Park[b], Kiwon Cho[b], Young Woo Park[b], Min Guo[c], Weiwei He[d], Xiang-Lei Yang[d], Paul Schimmel[d,1], and Sunghoon Kim[a,e,1]

[a]Medicinal Bioconvergence Research Center, and [e]World Class University Department of Molecular Medicine and Biopharmaceutical Sciences, Graduate School of Convergence Technology, Seoul National University, Seoul 151-742, Korea; [b]Integrative Omics Research Center, Korea Research Institute of Bioscience and Biotechnology, Daejeon 305-806, Korea; [c]Department of Cancer Biology, The Scripps Research Institute, Jupiter, FL 33458; and [d]The Skaggs Institute for Chemical Biology and Department of Molecular Biology, The Scripps Research Institute, La Jolla, CA 92037

Contributed by Paul Schimmel, January 10, 2012 (sent for review September 27, 2011)

Although adaptive systems of immunity against tumor initiation and destruction are well investigated, less understood is the role, if any, of endogenous factors that have conventional functions. Here we show that glycyl-tRNA synthetase (GRS), an essential component of the translation apparatus, circulates in serum and can be secreted from macrophages in response to Fas ligand that is released from tumor cells. Through cadherin (CDH)6 (K-cadherin), GRS bound to different ERK-activated tumor cells, and released phosphatase 2A (PP2A) from CDH6. The activated PP2A then suppressed ERK signaling through dephosphorylation of ERK and induced apoptosis. These activities were inhibited by blocking GRS with a soluble fragment of CDH6. With in vivo administration of GRS, growth of tumors with a high level of CDH6 and ERK activation were strongly suppressed. Our results implicate a conventional cytoplasmic enzyme in translation as an intrinsic component of the defense against ERK-activated tumor formation.

cytokine | proapoptotic effect | immune surveillance | cancer microenvironment

As ancient proteins that arose as part of the development of the genetic code, aminoacyl-tRNA synthetases (AARSs) are essential components of the translation apparatus. The 20 enzymes, 1 for each amino acid, catalyze the attachment of each amino acid to its cognate tRNA in the cytoplasm, where the charged tRNAs are then used for ribosomal protein synthesis (1). Surprisingly, ex-translational functions have been discovered for many tRNA synthetases, including gene regulation in *Escherichia coli*, RNA splicing in mitochondria of *Neurospora crassa* (2), and a diverse variety of functions in vertebrates that include among others regulation of inflammatory responses and of angiogenesis (3). These expanded functions are associated with the accretive additions of specialized motifs and domains—such as internal short sequence motifs and appended GST, leucine zipper, and helix-turn-helix domains (4). The specialized motif and domain additions facilitate new protein–protein interactions that confer novel functions. Some of the many disease connections to AARSs, and to proteins that are part of the multi-tRNA synthetase complex in mammalian cells, are thought to result from disruptions to, or alterations of, their ex-translational functions (5, 6). Indeed, there are dominant Charcot–Marie–Tooth disease-causing mutations in tyrosyl- and glycyl-tRNA synthetases that do not disrupt aminoacylation activity (7, 8).

Also surprising for essential components of the translation apparatus was the observation that specific fragments (produced by alternative splicing or natural proteolysis) of tyrosyl- and tryptophanyl-tRNA synthetases (YRS and WRS) bind to and signal through extracellular receptors, including chemokine receptor 1 and 2 (CXCR1 and -2) on polymorphonuclear leukocyte (PMN) cells (YRS) (9) and vascular endothelial (VE)-cadherin on endothelial cells (WRS) (10). These two synthetases are secreted from mammalian cells under specific conditions that potentiate their ex-translational functions (11, 12). Collectively, these observations raised the possibility that one way to discover ex-translational functions of tRNA synthetases might be by annotating those that were present in a physiological setting that did not carry out translation. This consideration led us to examine the presence of specific synthetases in human serum. Among other factors, we considered the "antisynthetase syndrome," namely, the observation that 30% of all autoimmune patients, including those with idiopathic inflammatory myopathies, rheumatoid arthritis, and interstitial lung disease, have autoantibodies directed against one of seven specific tRNA synthetases (13–15). Among other explanations, we considered the possibility that one or more of these seven synthetases might normally circulate as antigens having specific extracellular functions (16). Interestingly, glycyl-tRNA synthetase (GRS) autoantibodies were also detected in serum of patients with cancer (17). In part because of our ongoing investigations of its novel functions, we focused on GRS. Interestingly, in preliminary experiments, we detected GRS in the serum of normal human subjects and the mouse. These observations led us to attempt to understand a potential role for GRS as a secreted protein in a cancer microenvironment.

Results

Secretion of GRS from Macrophages. GRS was detected in the serum of three different human subjects and of two different CL57BL/6 mice (*SI Appendix*, Fig. S1*A*). Consistent with a lack of cell lysis, neither β-tubulin, nor lactate dehydrogenase (LDH), nor GAPDH was detected in the same sample. To have clues to the physiological function of secreted GRS, we examined whether secretion of GRS could be detected from cultured cells and, if so, whether such secretion was specific to a cell type. Six different cell lines (H322, A549, HEK293, HCT116, RAW 264.7, and HeLa) were incubated in a serum-free medium for 12 h, and the secreted proteins were precipitated from the medium using trichloroacetic acid (TCA). The precipitated proteins were determined by Western blot analysis with anti-human cytoplasmic GRS polyclonal antibody (α-GRS). Among the six tested cell lines, GRS was detected only in the culture medium of murine macrophage cell line RAW 264.7 (*SI Appendix*, Fig. S1*B*). Under the same conditions, we observed no release of tubulin into the medium, suggesting that the presence of GRS in the medium was not due to cell lysis (*SI Appendix*, Fig. S1*B*).

Author contributions: M.C.P., P.S., and S.K. designed research; M.C.P., T.K., D.J., J.M.H., S.B.K., Y.J.P., K.C., and W.H. performed research; M.C.P., J.M.H., Y.W.P., M.G., X.-L.Y., P.S., and S.K. analyzed data; and M.C.P., P.S., and S.K. wrote the paper.

The authors declare no conflict of interest.

[1]To whom correspondence may be addressed. E-mail: schimmel@scripps.edu or sungkim@snu.ac.kr.

See Author Summary on page 4035 (volume 109, number 11).

This article contains supporting information online at www.pnas.org/lookup/suppl/doi:10.1073/pnas.1200194109/-/DCSupplemental.

For RAW 264.7 cells, a significant amount of secreted GRS was detected in the medium after 12 h of starvation (*SI Appendix*, Fig. S1*C*). Given the specificity of GRS secretion, we investigated other immune cells, such as human T lymphocyte Jurkat cells, murine microglia-derived BV2 cells, and human macrophage-like U937 monocytes. Secretion of GRS was detected only in U937 as well as RAW 264.7 cells, but not in Jurkat or BV2 cells (*SI Appendix*, Fig. S1*D*). Thus, GRS was secreted from macrophages/monocytes under starvation conditions.

Different Apoptotic Stresses Induce Secretion of GRS. To investigate whether GRS secretion can be induced by stimuli other than starvation, we treated RAW 264.7 cells with signaling molecules. The signaling molecules included estrogen, which regulates cytokine production in macrophages (18); TNF-α, which influences macrophage differentiation (19); and EGF, which can be secreted from macrophages and tumor cells. In addition, we tested Adriamycin to induce cell death through DNA damage. Among these four "ligands", only Adriamycin induced secretion of GRS (*SI Appendix*, Fig. S2*A*), suggesting that apoptotic stress was important for GRS secretion. We then treated RAW 264.7 cells with other apoptotic stresses and compared the time course of GRS secretion. In addition to Adriamycin, both glucose deprivation and treatment with TNF-α with cycloheximide resulted in time-dependent secretion of GRS from RAW 264.7, but not from human colon cancer HCT 116 or cervical cancer HeLa cells (*SI Appendix*, Fig. S2*B*). These three apoptotic stresses also induced GRS secretion from U937 cells (*SI Appendix*, Fig. S2*C*). In contrast to GRS, no secretion of lysyl-tRNA synthetase (KRS) or YRS, other known AARS cytokines, was detected in Adriamycin-treated U937 cells (*SI Appendix*, Fig. S2*D*).

Because GRS secretion was observed immediately after the onset of any of three different apoptotic stresses, it is unlikely that secretion of GRS resulted from cell lysis. To confirm this conclusion, we determined cell lysis by monitoring the population of the sub-G1 cells, which reflect those apoptotic cells with hypodiploid DNA content resulting from DNA degradation, and by performing a 3-(4,5-dimethylthiazol-2-Yl)-2,5-diphenyltetrazolium bromide (MTT) assay. We found that none of the apoptotic stresses seriously affected cell cycle and viability (*SI Appendix*, Fig. S3 *A* and *B*). We also measured the activity of cytosolic LDH. The LDH activity in the medium was <10% of that in the cell extracts and did not increase in the conditioned medium (*SI Appendix*, Fig. S3*C*). Because cell membrane integrity is disrupted in apoptosis or necrosis, we stained RAW 264.7 cells with membrane-permeable Yo-Pro and also with membrane-impermeable propidium iodide (20). Neither dye stained the nuclear structure after induction of apoptotic stresses. However, both dyes stained nuclear DNA when macrophages were irradiated with UV (200 J/m^2) for 18 h (*SI Appendix*, Fig. S3*D*). These results are consistent with GRS secretion not arising from cell lysis or membrane rupture.

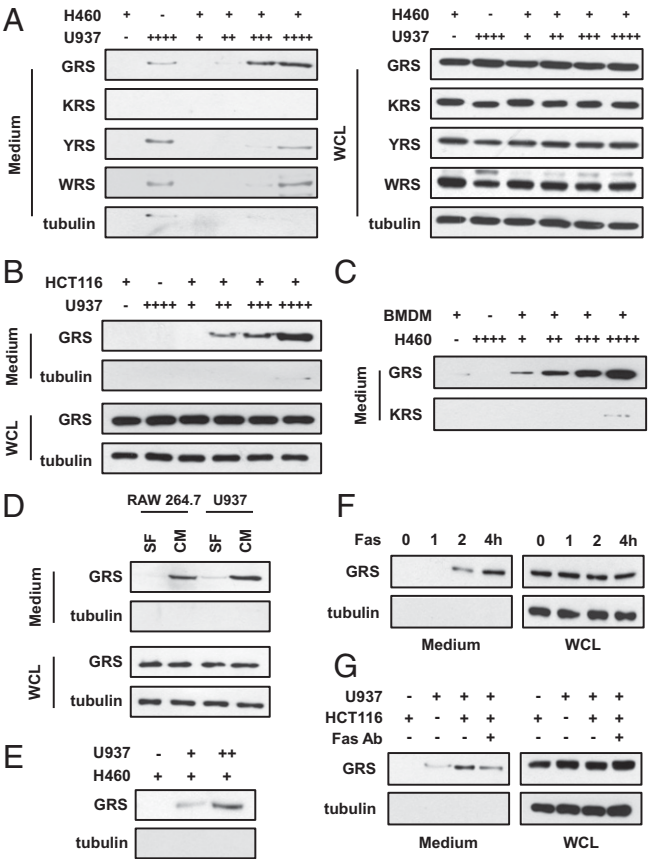

Fig. 1. GRS secretion can be induced by a Fas ligand signal derived from cancer cells. (*A*) H460 cancer cells were first seeded (0.25 × 10^6 cells/well). After 12 h, the medium was changed with serum-free medium and the cells were cocultured with U937 monocytes (0.125 × 10^6– ~1 × 10^6 cells per well) for 6 h. Then, secretion of GRS in the cultured medium was determined by TCA precipitation of proteins followed by SDS/PAGE and Western blot analysis. (*B*) Cocultivation of HCT116 cancer cells with U937 cells and determination of GRS secretion were determined as stated above. (*C*) Bone-marrow–derived macrophage (BMDM) and H460 cells were coincubated and GRS secretion was monitored. (*D*) The cultured medium of H460 cells was harvested after 12 h incubation and used as the conditioned medium (CM) for RAW 264.7 and U937 cells for 6 h. The secretion of GRS was determined as above. (*E*) H460 cells were incubated in a Transwell chamber with or without U937 cells in the insert for 6 h in serum-free medium and the secretion of GRS was analyzed. (*F*) U937 cells were treated with activating anti-Fas antibody (CH11 clone, 5 μg/mL) at the indicated times and the secretion of GRS was determined. (*G*) Neutralizing anti-Fas antibody (ZB4 clone, 0.2 μg/mL) was added to the medium of the coculture system and GRS secretion was determined as above. Molecular mass of examined proteins: GRS, 79 kDa; KRS, 72 kDa; YRS, 51 kDa; WRS, 53 kDa; and tubulin, 50 kDa.

GRS Secretion Can Be Induced by Fas Ligand Derived from Cancer Cells. Macrophages play a critical role in immune surveillance of the cancer cell microenvironment. To explore whether the secretion of GRS from macrophages was affected by proximity to tumor cells, we set up a coculture system with H460 human large cell lung tumor and U937 cells. Secretion of GRS, but not KRS, YRS, and WRS, was observed and the amount of secretion increased as the number of added U937 cells was increased (Fig. 1*A*).

GRS secretion was also detected in the coculture systems with HCT116 and U937 cells (Fig. 1*B*). To further confirm that GRS secretion also occurs in primary cells, we isolated and used murine bone marrow-derived macrophages (BMDMs) and incubated them with H460 cells. In this coculture system, GRS was also secreted from BMDMs, indicating that GRS secretion can take place in nontransformed macrophages (Fig. 1*C*). Next, to determine whether GRS secretion required physical contact between tumor and macrophage cells, we used conditioned medium and Transwell culture dishes as described previously (21). Conditioned medium harvested from H460 cells induced GRS secretion from RAW 264.7 and U937 cells (Fig. 1*D*). We also separated U937 and H460 cells by incubating U937 cells in the inserts and H460 cells in the chambers of Transwell dishes. Secretion of GRS increased according to the number of U937 cells (Fig. 1*E*). These results suggest that secretion of GRS does not require physical contact between cancer and macrophage cells.

Because tumor cells can escape immune surveillance by secreting Fas ligand (22), we examined whether Fas ligand was involved in GRS secretion. To test this possibility, we added agonistic Fas antibody to U937 cells and determined whether this addition triggered secretion of GRS. Indeed, after the treatment, GRS

accumulated in the medium in a time-dependent way (Fig. 1*F*). To confirm the correlation between Fas ligand and GRS secretion, we added an antagonistic Fas antibody to the coculture system. After the neutralizing effect, GRS secretion was decreased (Fig. 1*G*). These results are consistent with a model of GRS being secreted by Fas ligand derived from cancer cells.

Cell Binding of Secreted GRS. To determine the target cells of the secreted GRS, we incubated MCF7 (human breast cancer), HeLa, HCT116, and RAW 264.7 cells with different concentrations of biotinylated GRS. With this assay, biotinylated GRS was detected as bound to HCT116, HeLa, and RAW 264.7 cells in a dose-dependent manner, but not to MCF7 cells (Fig. 2*A*). Next, we determined the time course of GRS binding to HeLa and HCT116 cells. Binding of biotinylated GRS was detected after 5 min of incubation with these cells and increased to a maximum at 15–30 min (*SI Appendix*, Fig. S4*A*). To confirm the specificity of cell binding by GRS, the cells were preincubated with unlabeled GRS, after which biotinylated GRS was added. The biotin signal was significantly suppressed when the cells were pretreated with unlabeled GRS (*SI Appendix*, Fig. S4*B*). Cell binding of GRS was further monitored by immunofluorescence staining. Biotinylated GRS was incubated with HCT116 cells and cell-bound GRS was reacted with Alexa488-conjugated streptavidin. The staining intensity increased according to the amount of GRS, but was reduced by the addition of unlabeled GRS (*SI Appendix*, Fig. S4*C*); thus, the staining intensity was specifically attributable to GRS binding. Collectively our results show that specific tumor cells and macrophages are targets of secreted GRS.

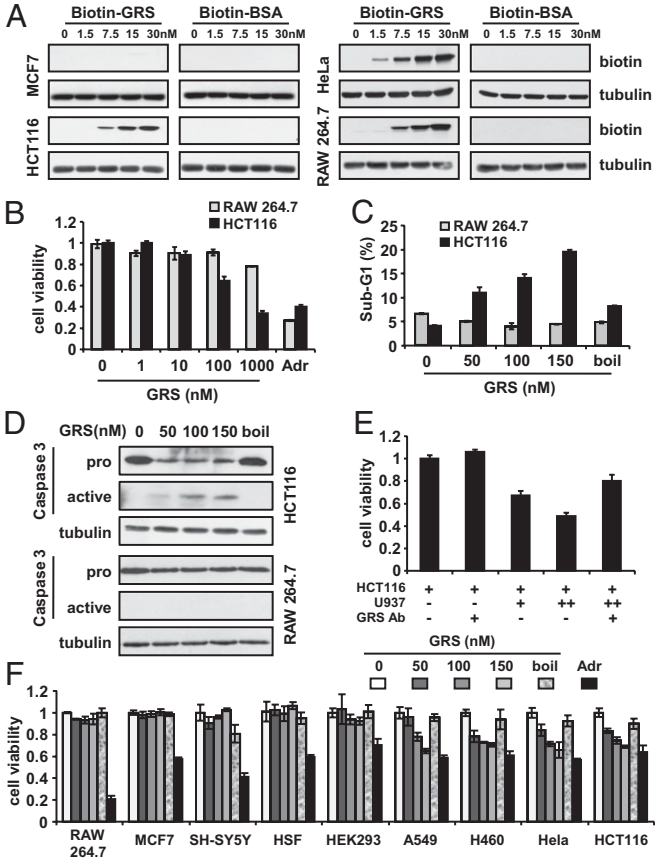

Fig. 2. Secreted GRS induces apoptosis in several different tumor cells. (*A*) Dose-dependent binding of biotinylated GRS was determined with MCF-7, HeLa, HCT116, and RAW 264.7 cell lines by capture with streptavidin-HRP. (*B*) RAW 264.7 and HCT116 cells were treated with the indicated concentrations of recombinant human GRS for 24 h and the cell viability was measured by the MTT assay. Adriamycin (2 μg/mL) was used as a positive control to induce cell death. (*C*) The effect of GRS on cell death was also monitored by sub-G1 cells, using flow cytometry. GRS (150 nM) was boiled to see whether it can inactivate the cytokine activity. (*D*) GRS-induced cell death was also monitored by the generation of active caspase 3. (*E*) Using a Transwell, U937 cells were incubated in the insert with or without HCT116 in the chamber (for 24 h) and cell viability was analyzed as above. To neutralize the effect of GRS, anti-GRS antibody was added to the culture dish. (*F*) Nine different cell lines were treated with the indicated concentrations of GRS and the effect on cell viability was determined by the MTT assay. Error bars give the mean ± SD from the average of three experiments. Molecular mass of examined proteins: procaspase 3, 32 kDa; and active-caspase 3, 17 kDa.

Proapoptotic Effect of GRS on Tumor Cells. Given that GRS secretion is induced by apoptotic ligands such as Fas, which are secreted from tumor cells, and that secreted GRS binds to tumor cells, we investigated whether GRS exerted a paracrine effect. We monitored cell viability and death by using an MTT assay and flow cytometry, respectively. When treated with GRS, the viability of HCT116, but not of RAW 264.7 cells, decreased in a dose-dependent manner (Fig. 2*B*). The sub-G1 population of HCT116, but not of RAW 264.7 cells, was also increased by treatment with GRS (Fig. 2*C*). GRS treatment resulted in the activation of caspase 3 (Fig. 2*D*) and also enhanced the release of cytochrome *c*, both of which are the known signatures of cell death (*SI Appendix*, Fig. S4*D*). Because heat-inactivated GRS did not exert any proapoptotic effects in these assays (Fig. 2 *C* and *D*), the native conformation of GRS appears to be important for its proapoptotic activity.

To investigate whether GRS can induce cell death in a physiological environment, we cocultured HCT116 and U937 cells by using Transwell chambers with or without α-GRS. The viability of HCT116 cells decreased on cocultivation with U937 cells. However, the addition of α-GRS compromised the effect of GRS on the viability of HCT116 (Fig. 2*E*). In further experiments, GRS reduced the viability of different tumor cell lines, including A549 (human alveolar adenocarcinoma), H460, HCT116, and HeLa cells. However, GRS had no effect on the viability of MCF-7 or human neuroblastoma SH-SY5Y cells or on the viability of human skin fibroblasts (HSF), human embryonic kidney HEK293 cells, or RAW 264.7 cells (Fig. 2*F*). Thus, GRS exerts its proapoptotic activity on a specific set of cancer cells.

Cadherin-6 As a Functional Receptor for GRS. Given that the secreted N-terminal–truncated WRS binds to VE-cadherin to inhibit angiogenesis (10) and that several cadherins (CDHs) are known to be associated with tumor cell survival and malignancy (23), we tested whether GRS can bind to any of 11 different CDH proteins. The interaction of His-GRS with the extracellular domains of 11 different cadherins individually fused to the Fc fragment of human IgG1 was determined by ELISAs. This screening identified specific binding of GRS to CDH6 and CDH18, but not to the remaining CDHs (Fig. 3*A*). GRS binding to CDH6 and CDH18, but not to CDH2, was confirmed by an in vitro pull-down assay (Fig. 3*B*). The binding affinity of GRS to CDH6 and -18 was measured by surface plasmon resonance assay. GRS bound to CDH6 and CDH18 with a K_d = 3.4 and 1.25 nM, respectively (Fig. 3*C* and *SI Appendix*, Fig. S5*A*), but not to IgG protein (*SI Appendix*, Fig. S5*B*).

Because CDH6 appears to be implicated in the etiology of hepatocellular carcinoma, renal carcinoma, and small cell lung cancer (SCLC) (24, 25), we investigated whether CDH6 can act as a functional receptor for GRS in tumor cells. First we determined the protein expression level of CDH6 in the tested tumor cell lines. We found that CDH6 expression was up-regulated in the GRS-sensitive cancer cell lines (HCT116, H460, and HeLa), but not in GRS-insensitive cancer cell lines (MCF7 and SH-SY5Y) (Fig. 3*D*). Using Western blot analysis and flow cytometry, we found that GRS binding to HCT116 cells was reduced when the CDH6 transcript was suppressed by its specific

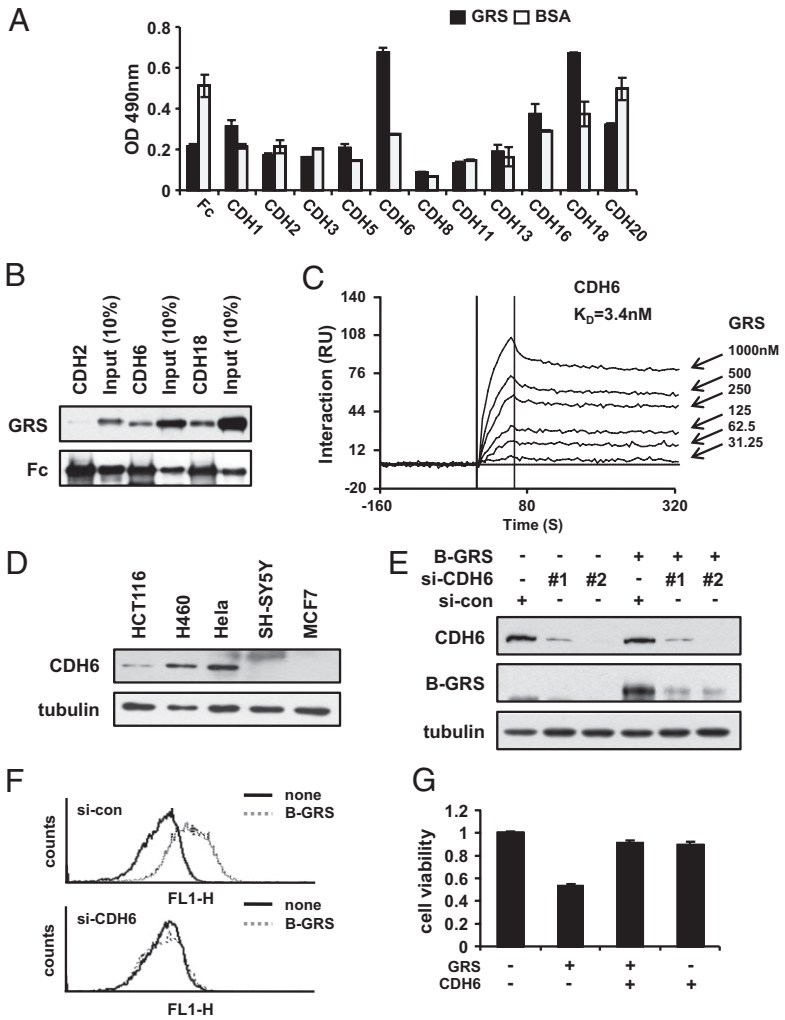

Fig. 3. Identification of CDH6 as a potential receptor for GRS. (*A*) A panel of Fc-fused soluble cadherin family proteins was bound to His-tag–fused GRS or to BSA-coated plates, and complexes were detected with the IgG_1 Fc-HRP reagent. (*B*) To confirm the binding between cadherins and GRS, Fc-CDH2, -6, and -18 were incubated with His-GRS. Fc-CDHs were precipitated with protein A/G agarose and coprecipitated GRS was determined by immunoblotting. (*C*) To calculate the equilibrium dissociation constant (K_d), immobilized Fc-fused (to gold chips) cadherins were incubated with GRS (31.25 nM– ~1000 nM). Binding of GRS to CDH6 was determined by surface plasmon resonance and expressed as resonance units (RU). (*D*) Five different cancer cells were determined for the expression of CDH6 by immunoblotting. (*E*) HCT116 cells were transfected with nonspecific siRNA controls or two differently designed siRNAs targeting CDH6 and treated with biotinylated GRS (15 nM), and the binding of GRS was analyzed by immunoblotting. (*F*) HCT116 cells were transfected with si-con and si-CDH6 as described above, and cell binding of GRS was measured by FACS analysis. (*G*) HCT116 cells were incubated with His-GRS (150 nM). To neutralize the effects of GRS, Fc-fused CDH6 (300 nM) was added and the cell viability was determined by the MTT assay. Error bars represent SD. Molecular mass of examined proteins: CDH6, 90 kDa; Fc-CDH2, 80 kDa; Fc-CDH6, 80 kDa; and Fc-CDH18, 78 kDa.

siRNA, but not by a nonspecific control siRNA (Fig. 3 *E* and *F* and *SI Appendix*, Fig. S5*C*). We then tested whether the soluble extracellular domain of CDH6 could offset the apoptotic activity of GRS. The effect of GRS on the viability of HCT116 cells was diminished by the addition of soluble CDH6 receptor protein (Fig. 3*G*). Our results suggest CDH6 is a functional receptor for GRS in tumor cells.

GRS Induces Cell Death via Suppression of ERK Activation. To investigate the mechanism by which GRS treatment induces cell death, we treated HCT116 cells with GRS and determined the effect on three mitogen-activated protein kinases: ERK, p38 MAPK, and JNK. The levels of phosphorylated ERK and p38 MAPK, but not JNK, were decreased by GRS treatment in a dose- and time-dependent manner (Fig. 4*A* and *SI Appendix*, Fig. S6*A*). Because activation of ERK is involved in cancer cell proliferation and survival (26), we tested whether the apoptotic susceptibility of cancer cells to GRS is determined by the activation status of ERK. GRS-sensitive HCT116, H460, and HeLa cancer cells showed enhanced phosphorylation of ERK, whereas GRS-insensitive SH-SY5Y and MCF7 cancer cells did not (Fig. 4*B*). This result provided a positive correlation between the activity of ERK and the sensitivity to GRS.

Among the three GRS-sensitive cell lines, HCT116 and H460 cells contain V-Ki-ras Kirstein rat sarcoma viral oncogene homolog (KRAS) mutations that lead to activation of ERK. The Ras-Raf-MEK-ERK cascade is a key signaling pathway for cancer cell proliferation and survival (27). We therefore tested whether activation of ERK by oncogenic Ras mutants renders apoptotic sensitivity to GRS treatment. For this purpose, we chose HEK293 cells that are normally insensitive to treatment with GRS. Three different Ras-active mutants [KRAS, V-Ha-ras Harvey rat sarcoma viral oncogene homolog (HRAS), and neuroblastoma RAS viral oncogene homolog (NRAS)] were introduced into HEK293 cells and stable cell lines were established. The selected stable cell lines showed increased phosphorylation of ERK. We treated the

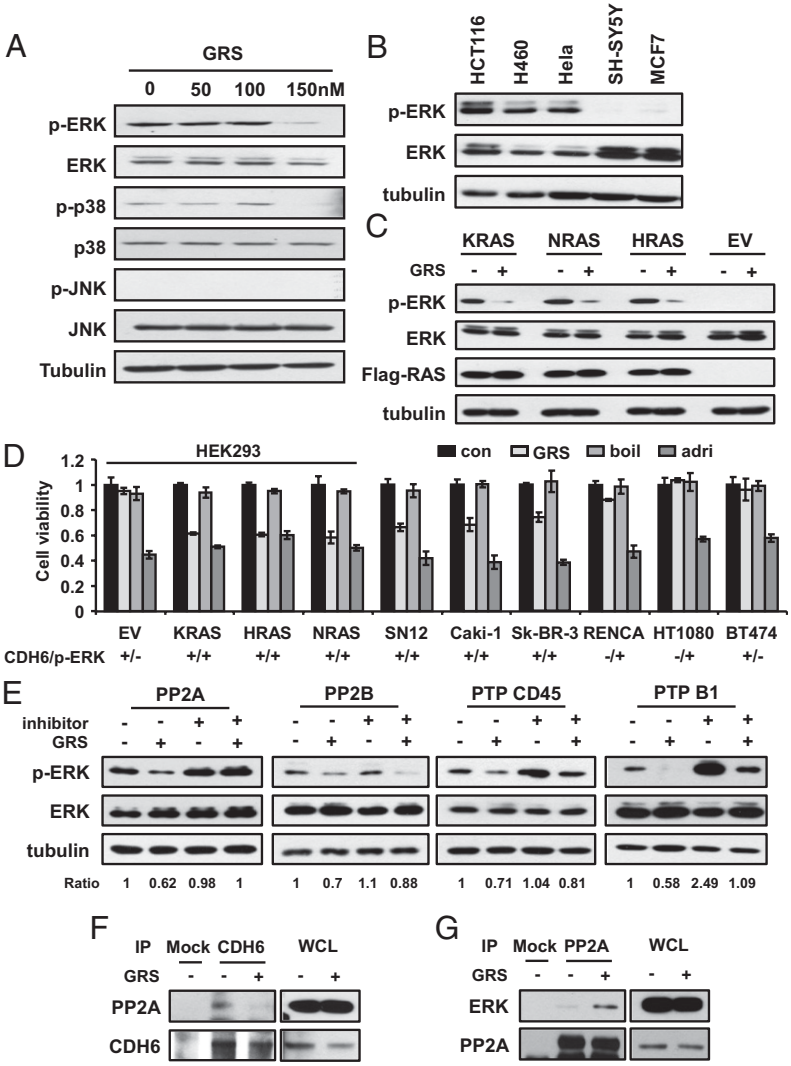

Fig. 4. Secreted GRS induces apoptosis of hyperphosphorylated ERK cancer cells. (*A*) HCT116 cells were treated with the indicated concentrations of GRS for 1 h and the phosphorylation of three different MAPKs was determined by their specific antibodies. (*B*) Five different cancer cell lines were investigated for the phosphorylation of ERK by immunoblotting. (*C*) HEK293 cells expressing each of three different active Ras transfectants were treated with GRS (150 nM) and its effect on the phosphorylation of ERK was determined as above. (*D*) Susceptibility of different cancer cell lines to GRS-induced cell death was determined by the MTT assay. Error bars give the mean ± SD from the average of three experiments. (*E*) HCT116 cells were treated with one of the inhibitors for PP2A, PP2B, PTP CD45, or PTP B1 for 15 min and incubated in the absence or presence of GRS (150 nM) for 1 h and phosphorylation of ERK was then determined. The bands of p-ERK and total ERK were quantified and the ratios of p-ERK to total ERK are shown. (*F*) The GRS effect on the interaction of CDH6 and PP2A was determined by coimmunoprecipitation in HCT116 cells. (*G*) HCT 116 cells were treated with GRS and its effect on the interaction of PP2A and ERK was determined by coimmunoprecpitation. Molecular mass of examined proteins: p-ERK, 42/44 kDa; ERK, 42/44 kDa; p-p38, 38 kDa; p38, 38 kDa; p-JNK, 46 kDa; JNK, 46 kDa; Flag-RASs, 22 kDa; and PP2A, 65 kDa.

cell lines with GRS and studied the effect on phosphorylation of ERK. In all three cell lines, GRS suppressed phosphorylation of ERK (Fig. 4*C*). GRS also increased the death of the three Ras transfectants but had no effect on the control HEK293 cells (Fig. 4*D* and *SI Appendix*, Fig. S6*B*). Our results are consistent with the hypothesis that, by the dephosphorylation of activated ERK, GRS can induce apoptosis of Ras-activated tumor cells.

We then examined whether the negative regulation of ERK phosphorylation by GRS-triggered CDH6 is universally applied to all cell types. Among the tested cell lines, HCT116, human renal carcinoma SN12, human breast carcinoma cell SK-BR-3, and human renal carcinoma Caki-1 showed high levels of both CDH6 and phosphorylated ERK (Fig. 4*D* and *SI Appendix*, Fig. S6*C*). However, the murine renal cancer cell line RENCA and the human fibrosarcoma cell line HT1080 showed high levels of ERK phosphorylation with undetectable levels of CDH6. In contrast, despite the high levels of CDH6, human breast carcinoma cell line BT474 showed low levels of ERK phosphorylation. In addition, transfection of HEK293 cells with K-, N-, and HRAS did not affect the cellular levels of CDH6 (*SI Appendix*, Fig. S6*D*). All of these results imply that the cellular level of CDH6 is not directly linked to the activation of ERK. We tested the susceptibility of the various cell lines to the apoptotic stress of administered GRS. Only cells with high levels of both CDH6 and ERK phosphorylation were susceptible to GRS-induced apoptosis (Fig. 4*D*).

Phosphorylation of ERK is regulated not only by the upstream MEK1 and -2 kinases, but also by phosphatases (28, 29). However, the phosphorylation of MEK was not reduced by GRS treatment (*SI Appendix*, Fig. S6*E*). To see whether GRS can suppress ERK phosphorylation by activating a phosphatase, we treated HCT116 cells with four different phosphatase inhibitors and checked how they would affect the GRS-induced de-

phosphorylation of ERK. Among them, the phosphatase 2A (PP2A) inhibitor, okadaic acid, specifically blocked GRS-dependent inhibition of ERK (Fig. 4*E*). GRS treatment also weakened the interaction between CDH6 and PP2A in HCT116 (Fig. 4*F*) and reduced the phosphorylation of PP2A (*SI Appendix*, Fig. S6*F*) to enhance the activity of PP2A (30, 31). Concomitantly, the interaction between PP2A and ERK was increased (Fig. 4*G*). These results suggest that GRS can release PP2A from CDH6 and induce PP2A activity, which then binds and dephosphorylates ERK.

Antitumor Effects of GRS in Vivo. To investigate the possibility that GRS may also be active in vivo, we tested GRS in a xenograft model using HCT116 cells. In the first experiments, HCT116 cells were s.c. injected into the right flank region of Balb/C nude mice, and tumors were grown to an average size of 100 mm^2. On day 9, either vehicle alone or 10 or 20 μg GRS was directly delivered to the tumors. Tumor volumes increased ~2.5-fold in the vehicle-treated group by day 21. In contrast, GRS injection reduced tumor volumes (Fig. 5 *A* and *B*) and weights (Fig. 5*C*) in a dose-dependent manner. The lack of change in animal weight and posture suggested no GRS-induced overt toxicity (Fig. 5*B* and *SI Appendix*, Fig. S7*A*). A higher number of Yo-Pro-1–positive tumor cells appeared in the GRS-treated tumor tissues than in the control tissues, suggesting the increased apoptosis by GRS (Fig. 5*D*).

Next, we examined the effect of GRS on the initial stage of tumorigenesis. HCT116 cells were injected into nude mice, with or without GRS (20 μg). Whereas tumor volumes increased up to 185 mm^2 in the vehicle control, tumors failed to grow when GRS

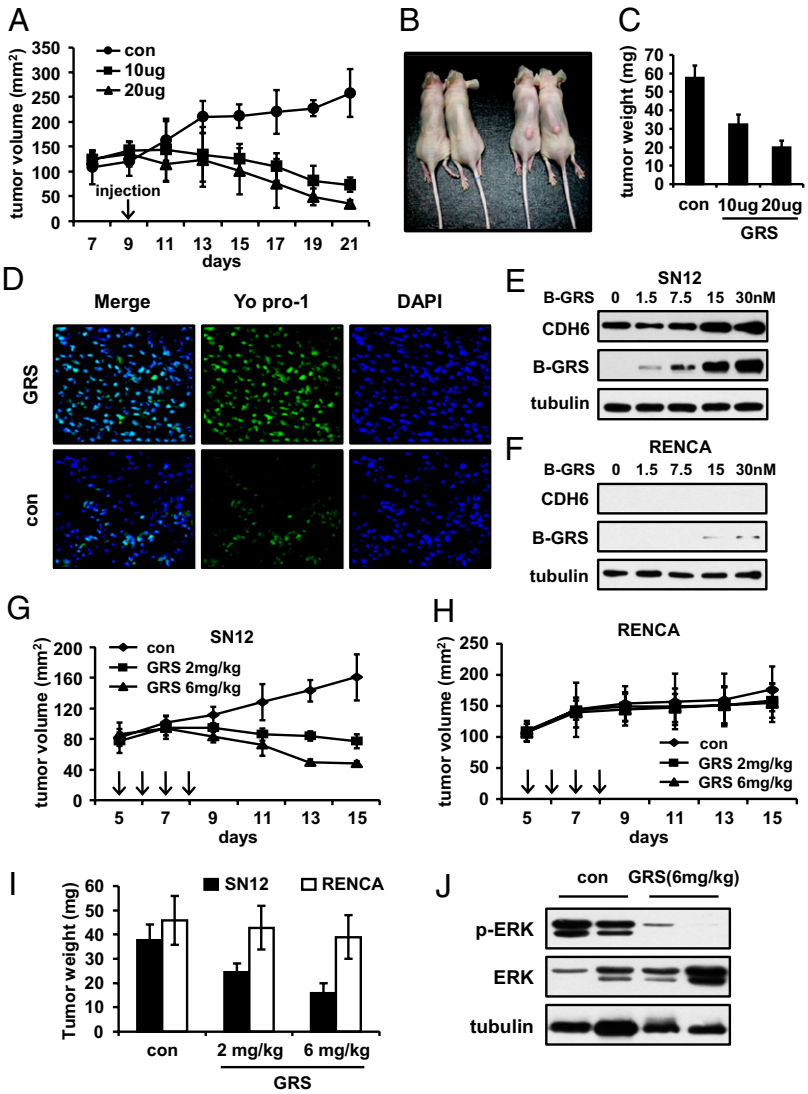

Fig. 5. Secreted GRS induces cancer cell death in vivo. (*A*) HCT116 cells were s.c. injected into the BALB/c nude mice and grown for 9 d. GRS (10 and 20 μg per dose) or PBS vehicle was intratumor injected ($n = 5$ animals per group). Tumor volume was calculated as the longest diameter × the shortest diameter^2 × 0.52. (*B*) Photograph of two representative HCT116 xenograft tumor mice from the control (*Right*) and treated (*Left*, 20 μg GRS) groups 12 d after the treatment. (*C*) Tumor weight was measured on the same day. (*D*) The OCT compound-embedded tissues were used for immunofluorescence staining. The tissues were treated with Yo-pro (green) and analyzed by immunofluorescence microscopy. Nuclei were stained with DAPI (blue). SN12 (*E*) and RENCA (*F*) cells were incubated with indicated concentrations of biotin-GRS (B-GRS) and the cell binding was determined by immunoblotting. SN12 (*G*) and RENCA (*H*) cells were s.c. injected into the BALB/c nude mice and grown for 5 d. GRS (2 and 6 mg/kg per dose) or PBS vehicle was i.p. injected daily for 4 d ($n = 5$ animals per group). Tumor volume was measured. (*I*) Tumor weights of the control and treated mice were determined and are shown as a bar graph. (*J*) The phosphorylation of ERK in SN12 xenograft tissues from the control and treated mice (6 mg/kg GRS) was determined by immunoblotting. Error bars give the mean ± SD.

was coinjected with the cells (*SI Appendix*, Fig. S7 *B–D*). Again, as evidenced by a lack of change in animal weight and posture, no overt toxicity due to the administration of GRS was observed (*SI Appendix*, Fig. S7 *C* and *E*). Apoptosis in HCT116 cells of the GRS-treated animals was clearly seen (*SI Appendix*, Fig. S7*F*).

To test whether antitumor activity of GRS in vivo is CDH6 dependent, we examined cell binding of GRS in renal cancer cells, SN12 and RENCA expressing high and low levels of CDH6, respectively. GRS bound only to SN12 cells, but not to RENCA cells (Fig. 5 *E* and *F*). We then transplanted SN12 and RENCA cells into nude mice and did four i.p. injections of GRS at two different doses (2 and 6 mg/kg). In these two models, GRS significantly inhibited the tumor volume and weight of SN12, but not of RENCA cells (Fig. 5 *G–I*). No GRS-induced toxicity occurred in both xenograft mouse models (*SI Appendix*, Fig. S7 *G* and *H*). In SN12 xenograft samples, dephosphorylation of ERK was clearly observed in the GRS treatment group (Fig. 5*J*), further validating the CDH6-dependent apoptotic activity of GRS.

Discussion

GRS is of increasing interest, not only because of its association with polymyositis, but also because of its causative role in Charcot–Marie–Tooth (CMT) disease (32, 33). Although it is not obvious whether the present work is in any way related to these diseases, proapoptotic activity of secreted GRS further implicates its functions beyond translation. In the case of two other circulating AARSs associated with polymyositis—asparaginyl-tRNA synthetase (NRS) and histidyl-tRNA synthetase (HRS)—cell migration-inducing interactions of each with CCR3 and CCR5 receptors on $CD4^+$ and $CD8^+$ T cells, immature dendritic cells and monocytes have been demonstrated (16). In the case of HRS, a connection of these activities to the etiology of polymyositis has been proposed (34). Although a similar analysis has not been carried out with GRS, the results with HRS and NRS establish a connection of at least two of the polymyositis-associated AARSs with the immune defense system. Thus, the longstanding observation of GRS being a prominent antigen in the serum of a specific subset of polymyositis patients may have some relationship to the results of this work, which suggest a role for GRS that is secreted from macrophages.

More specifically, GRS is implicated in the present work as being involved in immune surveillance against cancer. Previously reported antitumor cytokines include IFNs, IL-12, and TNF-related apoptosis-inducing ligand (TRAIL) that are secreted from antigen-presenting cells, T cells, and NK cells (35, 36). Although IFN-γ may also induce nonspecific cell death, TRAIL can induce cancer-specific cell death (37, 38). However, although macrophages play an important role in immune surveillance, no cytotoxic cytokine of macrophages has yet been identified. This work suggests that GRS is secreted by macrophages and acts as a cytokine with a distinct role against specific tumor cells, by decreasing phosphorylation of ERK via an interaction with CDH6.

The specific immune surveillance activity of GRS suggests its therapeutic potential against tumorigenesis. In many cancers, Ras is mutated to maintain a constitutively active status, thereby promoting cancer cell growth, survival, and migration. Significantly, tumor cells with activated Ras also engender highly activated ERK (39, 40). Our data suggest that secreted extracellular GRS is an intrinsic endogenous barrier for tumor initiation by activated Ras tumor cells and works by suppressing the activation of ERK.

Several cadherins are up-regulated in invasive cancer cells (23). Although expression of CDH6 has been reported in renal and lung cancers and in hepatocellular carcinoma (24, 25, 41), the function of CDH6 in cancer development and the identity of its natural ligand remain open questions. Adhesion molecules, including β1-integrin of T cells and vinexin-β of cancer cells, are known to regulate activation of ERK by protein phosphatases (42, 43). Here we showed that binding of GRS to CDH6 releases suppressed PP2A that dephosphorylates activated ERK.

CDH6 is a classic type II cadherin composed of five extracellular cadherin repeats (CR1–5) that promote calcium-dependent cell–cell adhesion. For the CDH family, the pairwise sequence identity of the extracellular domains varies from 27% to 68%, with the strong identity being between CDH6 and CDH18 (54%) (*SI Appendix*, Fig. S8*A*). The portions of the sequences that are specific to CDH6 and CDH18, and not shared by other cadherins, are spread across the extracellular region and mostly are in cadherin repeats (CRs) that are close to the transmembrane region (*SI Appendix*, Fig. S8*B*). Appearance of CDH6 and CDH18 happens at a late stage in evolution, as no classic types I and II (five CRs with a conserved intracellular domain) cadherins are found in *Caenorhabditis elegans* or *Drosophila melanogaster* (44, 45). Unlike the cadherin family members, α_2 homodimeric GRS is an essential protein distributed throughout all organisms in eukaryotes and archaea. It is likely that the evolution of CDH6 and -18 created a surface patch that matches to GRS for optimal binding. This phase of evolution of CDH6 and -18 may have been initiated at the time of appearance of extracellular GRS, at the stage of chordates or vertebrates (46).

The GRS–CDH6 complex now is the second demonstrated functional interaction [the first being the complex between secreted WRS and CDH5 (VE-cadherin)] (10) between a cadherin and an extracellular tRNA synthetase. Although the two synthetases bind cadherin family proteins, they appear to play distinct roles by recognizing different CR domains of different cadherins. For instance, direct binding of WRS to the CR1 domain of VE-cadherin may block the intercellular association of cadherins and prohibit cell adhesion. In contrast, binding of GRS to CDH6 triggers an intracellular event (presumably through the transmembrane segment) that induces dephosphorylation of activated ERK and apoptosis.

Renal cell carcinoma (RCC) annually accounts for >30,000 new cases and 12,000 deaths in the Unites States. RCC is characterized by the lack of early signs and results in metastasis at a high frequency. Metastatic RCC is often refractory to radiation and cytotoxic chemotherapy (47). In this case, novel target-based therapeutic agents are required. Genetic lesions affecting *Ras* or *EGFR* genes and activating ERK signaling have been observed in RCC (48, 49), and alterations of CDH6 expression are associated with the progression of RCC (25). SCLC accounts for ∼20% of the total lung cancer cases and is notorious for aggressive and chemoresistant characteristics (50). Adhesion-dependent activation of ERK signaling may contribute to chemoresistance of SCLC (51). From the therapeutic point of view, GRS can potentially be effective for treatment of metastatic RCC or SCLC in which CDH6 is highly expressed and the ERK pathway is active.

Materials and Methods

Protocols used in this study can be found in *SI Appendix, SI Methods*.

Coculture Assay. Coculture experiments were performed by inoculating U937 or RAW 264.7 cells (0.125×10^6– $\sim 1 \times 10^6$ cells/well) onto a layer of H460 or HCT116 cells (0.25×10^6/well) that had been cultured for 12 h in 6-well plates. The cells were then cocultured for 6 h in serum-free medium. To demonstrate whether a physical interaction between macrophages/monocytes and tumors in coculture was essential for GRS secretion, we used a 24-well Transwell cell culture chamber (Costar; 3470) fitted with inserts having 0.4-μm pores. H460 cells were seeded in the chambers, and U937 cells were seeded in the inserts and incubated separately at a 1:2 H460:U937 ratio for 12 h. The inserts were then transferred to the chambers in which the H460 cells were cultured. After 24 h in culture, the inserts were removed and the medium was harvested for assay of secretion.

ACKNOWLEDGMENTS. We thank Professor Lluis Ribas de Pouplana and Professor Frans Van Roy for their helpful comments on the manuscript. This work was supported in part by the Global Frontier (NRF-M1AXA002-2011-0028417) and Acceleration Research (R17-2007-020-01000-0) grants of the

National Research Foundation funded by the Ministry of Education, Science, and Technology of Korea; by National Institutes of Health Grants GM15539 and 23562 (to P.S.) and GM088278 (to X.-L.Y.); and by a fellowship from the National Foundation for Cancer Research.

1. Ibba M, Soll D (2000) Aminoacyl-tRNA synthesis. *Annu Rev Biochem* 69:617–650.
2. Kämper U, Kück U, Cherniack AD, Lambowitz AM (1992) The mitochondrial tyrosyl-tRNA synthetase of Podospora anserina is a bifunctional enzyme active in protein synthesis and RNA splicing. *Mol Cell Biol* 12:499–511.
3. Park SG, Ewalt KL, Kim S (2005) Functional expansion of aminoacyl-tRNA synthetases and their interacting factors: New perspectives on housekeepers. *Trends Biochem Sci* 30:569–574.
4. Guo M, Schimmel P, Yang X-L (2010) Functional expansion of human tRNA synthetases achieved by structural inventions. *FEBS Lett* 584:434–442.
5. Park SG, Schimmel P, Kim S (2008) Aminoacyl tRNA synthetases and their connections to disease. *Proc Natl Acad Sci USA* 105:11043–11049.
6. Sampath P, et al. (2004) Noncanonical function of glutamyl-prolyl-tRNA synthetase: Gene-specific silencing of translation. *Cell* 119:195–208.
7. Jordanova A, et al. (2006) Disrupted function and axonal distribution of mutant tyrosyl-tRNA synthetase in dominant intermediate Charcot-Marie-Tooth neuropathy. *Nat Genet* 38:197–202.
8. Nangle LA, Zhang W, Xie W, Yang X-L, Schimmel P (2007) Charcot-Marie-Tooth disease-associated mutant tRNA synthetases linked to altered dimer interface and neurite distribution defect. *Proc Natl Acad Sci USA* 104:11239–11244.
9. Wakasugi K, Schimmel P (1999) Two distinct cytokines released from a human aminoacyl-tRNA synthetase. *Science* 284:147–151.
10. Zhou Q, et al. (2010) Orthogonal use of a human tRNA synthetase active site to achieve multifunctionality. *Nat Struct Mol Biol* 17:57–61.
11. Wakasugi K, et al. (2002) A human aminoacyl-tRNA synthetase as a regulator of angiogenesis. *Proc Natl Acad Sci USA* 99:173–177.
12. Yang X-L, et al. (2007) Functional and crystal structure analysis of active site adaptations of a potent anti-angiogenic human tRNA synthetase. *Structure* 15: 793–805.
13. Mathews MB, Bernstein RM (1983) Myositis autoantibody inhibits histidyl-tRNA synthetase: A model for autoimmunity. *Nature* 304:177–179.
14. Mathews MB, Reichlin M, Hughes GR, Bernstein RM (1984) Anti-threonyl-tRNA synthetase, a second myositis-related autoantibody. *J Exp Med* 160:420–434.
15. Stojanov L, Satoh M, Hirakata M, Reeves WH (1996) Correlation of antisynthetase antibody levels with disease course in a patient with interstitial lung disease and elevated muscle enzymes. *J Clin Rheumatol* 2:89–95.
16. Howard OM, et al. (2002) Histidyl-tRNA synthetase and asparaginyl-tRNA synthetase, autoantigens in myositis, activate chemokine receptors on T lymphocytes and immature dendritic cells. *J Exp Med* 196:781–791.
17. Mun J, et al. (2010) A proteomic approach based on multiple parallel separation for the unambiguous identification of an antibody cognate antigen. *Electrophoresis* 31: 3428–3436.
18. Carruba G, et al. (2003) Estrogen regulates cytokine production and apoptosis in PMA-differentiated, macrophage-like U937 cells. *J Cell Biochem* 90:187–196.
19. Witsell AL, Schook LB (1992) Tumor necrosis factor alpha is an autocrine growth regulator during macrophage differentiation. *Proc Natl Acad Sci USA* 89:4754–4758.
20. Bhatnagar S, Shinagawa K, Castellino FJ, Schorey JS (2007) Exosomes released from macrophages infected with intracellular pathogens stimulate a proinflammatory response in vitro and in vivo. *Blood* 110:3234–3244.
21. Khodarev NN, et al. (2003) Tumour-endothelium interactions in co-culture: Coordinated changes of gene expression profiles and phenotypic properties of endothelial cells. *J Cell Sci* 116:1013–1022.
22. Igney FH, Krammer PH (2002) Immune escape of tumors: Apoptosis resistance and tumor counterattack. *J Leukoc Biol* 71:907–920.
23. Cavallaro U, Christofori G (2004) Cell adhesion and signalling by cadherins and Ig-CAMs in cancer. *Nat Rev Cancer* 4:118–132.
24. Shimazui T, et al. (1998) Expression of cadherin-6 as a novel diagnostic tool to predict prognosis of patients with E-cadherin-absent renal cell carcinoma. *Clin Cancer Res* 4: 2419–2424.
25. Shimoyama Y, Gotoh M, Terasaki T, Kitajima M, Hirohashi S (1995) Isolation and sequence analysis of human cadherin-6 complementary DNA for the full coding sequence and its expression in human carcinoma cells. *Cancer Res* 55:2206–2211.
26. Anjum R, Blenis J (2008) The RSK family of kinases: Emerging roles in cellular signalling. *Nat Rev Mol Cell Biol* 9:747–758.
27. Roberts PJ, Der CJ (2007) Targeting the Raf-MEK-ERK mitogen-activated protein kinase cascade for the treatment of cancer. *Oncogene* 26:3291–3310.
28. Keyse SM (2000) Protein phosphatases and the regulation of mitogen-activated protein kinase signalling. *Curr Opin Cell Biol* 12:186–192.
29. Wang PY, Liu P, Weng J, Sontag E, Anderson RG (2003) A cholesterol-regulated PP2A/HePTP complex with dual specificity ERK1/2 phosphatase activity. *EMBO J* 22: 2658–2667.
30. Chen J, Martin BL, Brautigan DL (1992) Regulation of protein serine-threonine phosphatase type-2A by tyrosine phosphorylation. *Science* 257:1261–1264.
31. Janssens V, Goris J (2001) Protein phosphatase 2A: A highly regulated family of serine/threonine phophatases implicated in cell growth and signalling. *Biochem J* 53: 417–439.
32. Seburn KL, Nangle LA, Cox GA, Schimmel P, Burgess RW (2006) An active dominant mutation of glycyl-tRNA synthetase causes neuropathy in a Charcot-Marie-Tooth 2D mouse model. *Neuron* 51:715–726.
33. Motley WW, Talbot K, Fischbeck KH (2010) GARS axonopathy: Not every neuron's cup of tRNA. *Trends Neurosci* 33:59–66.
34. Raben N, et al. (1994) A motif in human histidyl-tRNA synthetase which is shared among several aminoacyl-tRNA synthetases is a coiled-coil that is essential for enzymatic activity and contains the major autoantigenic epitope. *J Biol Chem* 269: 24277–24283.
35. Swann JB, Smyth MJ (2007) Immune surveillance of tumors. *J Clin Invest* 117: 1137–1146.
36. Trinchieri G (1995) Natural killer cells wear different hats: Effector cells of innate resistance and regulatory cells of adaptive immunity and of hematopoiesis. *Semin Immunol* 7:83–88.
37. Almasan A, Ashkenazi A (2003) Apo2L/TRAIL: Apoptosis signaling, biology, and potential for cancer therapy. *Cytokine Growth Factor Rev* 14:337–348.
38. Luo J-L, Maeda S, Hsu L-C, Yagita H, Karin M (2004) Inhibition of NF-kappaB in cancer cells converts inflammation-induced tumor growth mediated by TNFalpha to TRAIL-mediated tumor regression. *Cancer Cell* 6:297–305.
39. Bos JL (1989) ras oncogenes in human cancer: A review. *Cancer Res* 49:4682–4689.
40. Lange-Carter CA, Johnson GL (1994) Ras-dependent growth factor regulation of MEK kincase in PC12 cells. *Science* 2:1458–1461.
41. Scandurro AB, Weldon CW, Figueroa YG, Alam J, Beckman BS (2001) Gene microarray analysis reveals a novel hypoxia signal transduction pathway in human hepatocellular carcinoma cells. *Int J Oncol* 19:129–135.
42. Laakko T, Juliano RL (2003) Adhesion regulation of stromal cell-derived factor-1 activation of ERK in lymphocytes by phosphatases. *J Biol Chem* 278:31621–31628.
43. Mitsushima M, Ueda K, Kioka N (2007) Involvement of phosphatases in the anchorage-dependent regulation of ERK2 activation. *Exp Cell Res* 313:1830–1838.
44. Hill E, Broadbent ID, Chothia C, Pettitt J (2001) Cadherin superfamily proteins in Caenorhabditis elegans and Drosophila melanogaster. *J Mol Biol* 305:1011–1024.
45. Pettitt J (2005) The cadherin superfamily. *WormBook* 29:1–9.
46. Guo M, Yang X-L, Schimmel P (2010) New functions of aminoacyl-tRNA synthetases beyond translation. *Nat Rev Mol Cell Biol* 11:668–674.
47. Motzer RJ, Bander NH, Nanus DM (1996) Renal-cell carcinoma. *N Engl J Med* 335: 865–875.
48. Fujita J, et al. (1988) Activated H-ras oncogenes in human kidney tumors. *Cancer Res* 48:5251–5255.
49. Stumm G, et al. (1996) Concomitant overexpression of the EGFR and erbB-2 genes in renal cell carcinoma (RCC) is correlated with dedifferentiation and metastasis. *Int J Cancer* 69:17–22.
50. Aisner J (1996) Extensive-disease small-cell lung cancer: The thrill of victory; the agony of defeat. *J Clin Oncol* 14:658–665.
51. Sethi T, et al. (1999) Extracellular matrix proteins protect small cell lung cancer cells against apoptosis: A mechanism for small cell lung cancer growth and drug resistance in vivo. *Nat Med* 5:662–668.